Preparation of Mercury(II) Complexes of Tris[(2-pyridyl)methyl]amine and Characterization by X-ray Crystallography and NMR Spectroscopy

Deborah C. Bebout,* David E. Ehmann, Jonathan C. Trinidad, and Kathleen K. Crahan

Department of Chemistry, The College of William and Mary, Williamsburg, Virginia 23187

Margaret E. Kastner and Damon A. Parrish

Department of Chemistry, Bucknell University, Lewisburg, Pennsylvania 17837

Received March 7, 1997[⊗]

The complexation of Hg(II) by the tripodal ligand tris[(2-pyridyl)methyl]amine (TMPA) was investigated by solution state NMR and X-ray crystallography. Mercury coordination compounds exhibiting rarely observed room-temperature solution state NMR $^{1}H^{199}Hg$ and $^{13}C^{199}Hg$ satellites were characterized. Solvent, counterion, temperature, and concentration effects on solution state NMR properties were investigated. The solution state NMR were correlated with two solid state structures. The eight-coordinate complex $[Hg(TMPA)_2](ClO_4)_2$ (**1**) crystallizes in the monoclinic space group $P2_1/n$ with $a = 9.735(10)$ Å, $b = 10.963(2)$ Å, $c = 18.553(34)$ Å, $\beta = 103.81(12)°$, and $Z = 2$. The mercury is at the inversion center of a bicapped trigonal antiprism. The Hg−N_{amine} distance is 2.560(3) Å, and the average Hg−$N_{pyridyl}$ distance is 2.58(2) Å. The five-coordinate complex $[Hg(TMPA)Cl]_2(HgCl_4)$ (**2**) crystallizes in the triclinic space group $P\bar{1}$ with $a = 11.887(2)$ Å, $b = 13.260(2)$ Å, $c = 15.278(4)$ Å, $\alpha = 112.27(2)°$, $\beta = 109.39(2)°$, $\gamma = 90.670(10)°$, and $Z = 2$. The two crystallographically unique cations are distorted trigonal bipyramids. The average Hg−Cl distance is 2.355(12) Å, the average Hg−N_{amine} distance is 2.43(2) Å, and the average Hg−$N_{pyridyl}$ distance is 2.40(5) Å.

Introduction

Investigation of the coordination chemistry of Hg(II) is complicated by the tolerance for many different coordination numbers and coordination geometries. Numerous studies have demonstrated that, in spite of the high thermodynamic stability of Hg(II) complexes, Hg(II) is prone to rapid exchange in solution among the multitude of ligating groups that it encounters.[1] As a result, observation of satellites attributable to proton or carbon coupling to the $I = {}^1/_2$, 16.85% natural abundance ^{199}Hg nucleus has been rare for Hg(II) coordination compounds in solution.[2,3] Mercury has only one other NMR-active isotope, ^{201}Hg, and the large quadrupole moment of this nucleus prevents routine observation. Recent investigations of Hg(II)-substituted proteins have demonstrated that the multidentate coordination environment of proteins can establish slow-exchange conditions sufficient for observation of $^{1}H^{199}Hg$ coupling by solution state NMR methods.[3−5] Preliminary evidence suggesting $^{1}H^{199}Hg$ scalar coupling information could be applied to distance geometry-based structure refinement strategies was also obtained.[4] As an extension of this research, we have begun to investigate the Hg(II) coordination chemistry of synthetic polydentate ligands. Polydentate ligands are expected to geometrically and entropically restrict the number of accessible structures, but to a lesser degree than the well-defined metal binding sites of proteins.

Tripodal ligands have been applied extensively to the synthesis of metal complexes because of their ease of preparation, wealth of spectroscopic and X-ray crystallographic data available for their metal complexes, and the predictable changes in the physical properties of the metal complex with variation in the ligand. Coordination to a metal ion with favorable NMR properties provides an additional means of characterizing the dynamics of complexes in solution and correlating solution state spectra with solid state structures. The potentially tetradentate tripodal ligand TMPA (**3**, TMPA = tris[(2-pyridyl)methyl]-

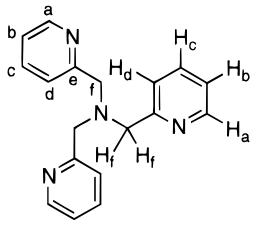

3

amine) was chosen for this study. The complexation of Hg(II) by tripodal ligands containing phosphorus and sulfur donor atoms has been examined extensively, and in select cases slow exchange in solution was observed.[2,3] However, we have been unable to identify any structurally characterized complexes of Hg(II) with tripodal ligands containing exclusively nitrogen donor atoms.

TMPA has been used to investigate the coordination chemistry of a wide variety of first-row transition-metal ions and alkali-metal ions. Metal ion affinities of TMPA for Hg(II) and a variety of other divalent metal ions have been measured.[6] TMPA complexes of Co(III),[7] Cr(III),[8] Cu(I),[9] Cu(II),[10] Fe(II),[11]

[⊗] Abstract published in *Advance ACS Abstracts,* August 15, 1997.

(1) Cheesman, B. V.; Arnold, A. P.; Rabenstein, D. L. *J. Am. Chem. Soc.* **1988**, *110*, 6359 and references cited therein.
(2) (a) Bashall, A.; McPartlin, M.; Murphy, B. P.; Powell, H. R.; Waikar, S. *J. Chem. Soc., Dalton Trans.* **1994**, 1383. (b) McWhinnie, W. R.; Monsef-Mirzai, Z.; Perry, M. C.; Shaikh, N. *Polyhedron* **1993**, *12*, 1193.
(3) Cass, A. E. G.; Galdes, A.; Hill, H. A. O.; McClelland, C. E.; Storm, C. B. *FEBS Lett.* **1978**, *94*, 311.
(4) Blake, P. R.; Lee, B.; Summers, M. F.; Park, J.-B.; Zhou, Z. H.; Adams, M. W. W. *New J. Chem.* **1994**, *18*, 387.
(5) Utschig, L. M.; Bryson, J. W.; O'Halloran, T. W. *Science* **1995**, *268*, 380.

S0020-1669(97)00277-2 CCC: $14.00

Fe(III),[12] Li(I),[13] Mn(II),[14,15] Mn(III),[16] Mn (IV),[16] Mo(II),[17] VO[18] and Zn(II)[19] have been structurally characterized. In these complexes, TMPA has served as both a tetracoordinate and tricoordinate ligand. Typically TMPA completes either five-coordinate trigonal bipyramidal or six-coordinate octahedral metal ion geometries; however, both four-coordinate and eight-coordinate metal ions have been observed in rare instances.

We report here the synthesis and characterization of two Hg(II) complexes of TMPA differing in stoichiometry. Significantly, conditions for slow exchange of Hg(II) in the solution state have been established which permit observation of $^{1}H^{199}Hg$ and $^{13}C^{199}Hg$ couplings by NMR. The solution spectra are correlated with the distinct solid state structures. The structures of the TMPA complexes are compared with other structurally characterized metal ion complexes of TMPA.

Experimental Section

Methods and Materials. Starting materials were of commercially available reagent quality unless otherwise stated. FT-IR spectra were recorded in KBr pellets on a Perkin-Elmer 1600. Elemental analyses were carried out by Atlantic Microlab, Inc., Norcross, GA.

All of the perchlorate salts of mercury(II) complexes included in this work were stable for routine synthesis and purification procedures. However, caution should be exercised because perchlorate salts of metal complexes with organic ligands are potentially explosive.[20]

Synthesis of Tris[(2-pyridyl)methyl]amine (TMPA, 3). The ligand TMPA was prepared by variation of the procedure described by Tyeklár and co-workers.[9] A solution of 2-picolyl chloride hydrochloride (23.5 g, 143.6 mmol) in 60 mL of deionized water was cooled to 0 °C. This solution was treated with 27 mL of 5.3 N aqueous NaOH. A solution of freshly distilled 2-(aminomethyl)pyridine (7.4 mL, 71.8 mmol) in 100 mL of dichloromethane was added rapidly dropwise with vigorous magnetic stirring to ensure mixing of the two phases. The mixture was allowed to warm to room temperature, and an additional 27 mL portion of 5.3 N aqueous NaOH was added over 48 h via syringe pump, ensuring that the pH did not exceed 9.5. The organic layer was separated from the mixture and washed with 60 mL of 2.5 N aqueous NaOH. The organics were dried with $MgSO_4$ and filtered. Following removal of the dichloromethane *in vacuo*, a 2 h Soxhlet extraction of the red-brown solid with diethyl ether provided a yellow solution, which was evaporated *in vacuo*. The waxy yellow solid was recrystallized from ether. Sublimation of the melted yellow solid (100 °C, 0.04 mmHg) yielded TMPA (3.7 g, 17.5%) as a white crystalline solid with mp 84−85 °C. ^{1}H NMR (CD_3CN): δ 8.47 (d, 3 H, J = 4 Hz, H_a), 7.69 (t, 3 H, J = 8 Hz, H_c), 7.59 (d, 3 H, J = 8 Hz, H_d), 7.18 (t, 3 H, J = 6 Hz, H_b), 3.81 (s, 6 H, H_f). ^{13}C NMR (CD_3CN): δ 160.54 (C_e), 150.06 (C_a), 137.36 (C_c), 123.79 (C_d), 123.03 (C_b), 60.87 (C_f). IR (KBr, cm^{-1}): 3077 w, 3051 w, 3013 w, pyridine C−H; 1590 s, 1569 s, pyridine C═N; 1474 s, 1446 sh, w, pyridine C═C; 1436 s, 1367 m, 1312 m, 1243 m, 1154 m, 1124 m, 1047 m, 982 m, 899 m, 767 m, 631 m, 606 m.

Synthesis of the Complex $[Hg(TMPA)_2](ClO_4)_2$ (1). Solid $Hg(ClO_4)_2 \cdot 3H_2O$ (0.31 g, 0.78 mmol) was added to a solution of the ligand TMPA (0.40 g, 1.38 mmol) in acetone (10 mL) with stirring. Colorless hexagonal plates of the complex (0.58 g, 81%) formed overnight with partial evaporation of solvent which were suitable for X-ray diffraction analysis. Mp: 190−191 °C. ^{1}H NMR (CD_3CN): δ 7.80 (t, 3 H, J = 7 Hz, H_c), 7.59 (b s, 3 H, H_a), 7.47 (t, 3 H, J = 8 Hz, H_d), 6.98 (b s, 3 H, H_b), 4.30 (s, 6 H, H_f). ^{13}C NMR (CD_3CN): δ 155.10 (C_e), 149.20 (C_a), 140.01 (C_c), 126.09 (C_d), 125.15 (C_b), 58.22 (C_f). IR (KBr, cm^{-1}): 3059 w, 3008 w, pyridine C−H; 1595 s, 1573 m, py C═N; 1478 m, 1435 m, pyridine C═C; 1088 vs, ClO_4; 1145 vs, 1118 vs, 1088 vs, 762 s, 636 m, 625 m. Anal. Calc for $C_{36}H_{36}Cl_2HgN_8O_8$: C, 44.11; H, 3.70; N, 11.43. Found: C, 44.04; H, 3.72; N, 11.50.

Synthesis of the Complex $[Hg(TMPA)Cl]_2(HgCl_4)$ (2). A solution of the ligand TMPA (0.35 g, 1.2 mmol) in acetonitrile (10 mL) was added to an acetonitrile solution (10 mL) of $HgCl_2$ (0.33 g, 1.2 mmol) with stirring. The complex (0.30 g, 52%) formed as pale yellow crystals suitable for X-ray diffraction analysis by slow evaporation. Mp: 162−163 °C. ^{1}H NMR (CD_3CN): δ 8.57 (d, 3 H, J = 5 Hz, H_a), 7.90 (t, 3 H, J = 8 Hz, H_c), 7.49 (t, 3 H, J = 5 Hz, H_b), 7.45 (d, 3 H, J = 7 Hz, H_d), 4.09 (s, 6 H, H_f). ^{13}C NMR (CD_3CN): δ 154.78 (C_e), 150.03 (C_a), 140.72 (C_c), 126.81 (C_d), 125.71 (C_b), 57.98 (C_f). IR (KBr, cm^{-1}): 3062 w, 3041 w, 3012 w, pyridine C−H; 1600 s, 1571 w, py C═N; 1480 m, 1437 m, 1431 m, pyridine C═C; 1372 m, 1313 m, 1295 m, 1262 m, 1151 m, 1095 m, 1051 m, 1013 m, 995 w, 985 w, 959 w, 895 w, 836 m, 787 m, 772 s, 754 m, 636 w. Anal. Calc for $C_{36}H_{36}Cl_6Hg_3N_8$: C, 31.00; H, 2.60; N, 8.03. Found: C, 31.26; H, 2.68; N, 8.12.

X-ray Crystallography. Selected crystallographic data are given in Table 1. Densities were measured by neutral buoyancy in bromoform/hexane solutions. Data were collected at room temperature on a Siemens R3 four-circle diffractometer using graphite-monochromated

Table 1. Selected Crystallographic Data

	$[Hg(TMPA)_2](ClO_4)_2$	$[Hg(TMPA)Cl]_2(HgCl_4)$
empirical formula	$C_{36}H_{36}N_8O_8Cl_2Hg$	$C_{36}H_{36}N_8Cl_6Hg_3$
fw	980.22	1395.20
crystal dimens, mm	0.5 × 0.2 × 0.2	0.40 × 0.30 × 0.13
crystal color and habit	colorless needle	colorless plate
crystal system	monoclinic	triclinic
space group	$P2_1/n$ (No. 14)	$P\bar{1}$ (No. 2)
a, Å	9.735(10)	11.887(2)
b, Å	10.963(2)	13.260(2)
c, Å	18.553(34)	15.278(4)
α, deg	90	112.27(2)
β, deg	103.81(12)	109.39(2)
γ, deg	90	90.670(10)
V, Å^3	1923(4)	2075.9(7)
Z	2	2
d_{calc}, Mg m^{-3}	1.69	2.23
d_{exp}, Mg m^{-3}	1.69	2.29
μ, mm^{-1}	4.2	11.5
R1	0.028	0.047
R2	0.082	0.14

(6) Anderegg, G.; Hubmann, E.; Podder, N. G.; Wenk, F. *Helv. Chim. Acta* **1977**, *60*, 123.
(7) Mandel, J. G.; Maricondi, C.; Douglas, B. E. *Inorg. Chem.* **1988**, *27*, 2990.
(8) (a) Hodgson, D. J.; Zietlow, M. H.; Pederson, E.; Toftlund, H. *Inorg. Chim. Acta* **1988**, *149*, 111−117. (b) Gafford, B. G.; Holwerda, R. A.; Schugar, H. J.; Potenza, J. A. *Inorg. Chem.* **1988**, *27*, 1126.
(9) Tyeklár, Z.; Jacobson, R. J.; Wei, N.; Murthy, N. N.; Zubieta, J.; Karlin, K. D. *J. Am. Chem. Soc.* **1993**, *115*, 2677.
(10) (a) Karlin, K. D.; Hayes, J. C.; Juen, S.; Hutchinson, J. P.; Zubieta, Z. *Inorg. Chem.* **1982**, *21*, 4106−4108. (b) Jacobson, R. R.; Tyeklar, Z.; Farooq, A.; Karlin, K. D.; Liu, S.; Zubieta, J. *J. Am. Chem. Soc.* **1988**, *110*, 3690. (c) Oshio, H.; Ichida, H. *J. Phys. Chem.* **1995**, *99*, 3294. (d) Komeda, N.; Nagao, H.; Kushi, Y.; Adachi, G.-y.; Suzuki, M.; Uehara, A.; Tanaka, K. *Bull. Chem. Soc. Jpn.* **1995**, *68*, 581.
(11) (a) Yan, S.; Cox, D. D.; Pearce, L. L.; Juarez-Garcia, C.; Que, L., Jr.; Zhang, J. H.; O'Connor, C. J. *Inorg. Chem.* **1989**, *28*, 2509. (b) Zang, Y.; Jang, H. G.; Chiou, Y.-M.; Hendrich, M. P.; Que, L., Jr. *Inorg. Chim. Acta* **1993**, *213*, 41.
(12) (a) Norman, R. E.; Yan, S.; Que, L., Jr.; Backes, G.; Ling, J.; Sanders-Loehr, J.; Zhang, J. H.; O'Connor, C. J. *J. Am. Chem. Soc.* **1990**, *112*, 1554. (b) Jang, H. G.; Cox, D. D.; Que, L., Jr. *J. Am. Chem. Soc.* **1991**, *113*, 9200. (c) Kojima, T.; Leising, R. A.; Yan, S.; Que, L., Jr. *J. Am. Chem. Soc.* **1993**, *115*, 11328. (d) Sasaki, Y.; Umakoshi, K.; Kimura, S.; Oh, C.-E.; Yamazaki, M.; Shibahara, T. *Chem. Lett.* **1994**, 1185.
(13) Brownstein, S. K.; Plouffe, P.-Y.; Bensimon, C.; Tse, J. *Inorg. Chem.* **1994**, *33*, 354.
(14) Oshio, H.; Ino, E.; Mogi, I.; Ito, T. *Inorg. Chem.* **1993**, *32*, 5697.
(15) Gultneh, Y.; Farooq, A.; Karlin, K. D.; Liu, S.; Zubieta, J. *Inorg. Chim. Acta* **1993**, *211*, 171.
(16) Towle, D. K.; Botsford, C. A.; Hodgson, D. J. *Inorg. Chim. Acta* **1988**, *141*, 167.
(17) Brisdon, B. J.; Cartwright, M.; Hodson, A. G. W.; Mahon, M. F.; Molloy, K. C. *J. Organomet. Chem.* **1992**, *435*, 319.
(18) Toftlund, H.; Larsen, S.; Murray, K. S. *Inorg. Chem.* **1991**, *30*, 3964.
(19) (a) Murthy, N. N.; Karlin, K. D. *J. Chem. Soc., Chem. Commun.* **1993**, 1236. (b) Adams, H.; Bailey, N. A.; Fenton, D. E.; He, Q.-Y. *J. Chem. Soc., Dalton Trans.* **1995**, 697.
(20) (a) Wosley, W. C. *J. Chem. Educ.* **1973**, *50*, A335. (b) Raymond, K. N. *Chem. Eng. News* **1983**, *61* (49), 4.

Table 2. Selected Bond Distances (Å) in $[Hg(TMPA)_2](ClO_4)_2$ and $[Hg(TMPA)Cl]_2(HgCl_4)$

$[Hg(TMPA)_2](ClO_4)_2$		$[Hg(TMPA)Cl]_2(HgCl_4)$	
Hg−N	2.560(3)	Hg(1)−N(A)	2.418(8)
		Hg(2)−N(B)	2.449(8)
Hg−N(1)	2.562(3)	Hg(1)−N(1)	2.399(8)
Hg−N(2)	2.595(4)	Hg(1)−N(2)	2.379(9)
Hg−N(3)	2.593(6)	Hg(1)−N(3)	2.390(9)
		Hg(2)−N(4)	2.323(9)
		Hg(2)−N(5)	2.463(9)
		Hg(2)−N(6)	2.409(9)
		Hg(1)−Cl(1)	2.346(3)
		Hg(2)−Cl(2)	2.363(3)
$N-C(F)_{av}$	1.466(5)	$N-C(F)_{av}$	1.50(3)
$N-C(A)_{av}$	1.334(8)	$N-C(A)_{av}$	1.33(3)
$N-C(E)_{av}$	1.332(4)	$N-C(E)_{av}$	1.35(2)
		$Hg-Cl_{av\ in\ anion}$	2.490(16)

Mo Kα X-radiation ($\lambda = 0.710\ 73$ Å) and the $\theta-2\theta$ technique over a 2θ range of 3−55°. During data collection, three standard reflections were measured after every 50 reflections. Both crystals turned black in the beam. The structures were solved by direct methods and Fourier difference maps using the SHELXTL-PLUS[21] package of software programs. Final refinements were done using SHELXL-93[22] minimizing $R2 = [\sum[w(F_o^2 - F_c^2)^2]/\sum[w(F_o^2)^2]]^{1/2}$, $R1 = \sum| |F_o| - |F_c| |/\sum |F_o|$, and $S = [\sum[w(F_o^2 - F_c^2)^2]/(n - p)]^{1/2}$. All non-hydrogen atoms were refined as anisotropic, and the hydrogen atomic positions were fixed relative to the bonded carbons and the isotropic thermal parameters were fixed.

Structure of $[Hg(TMPA)_2](ClO_4)_2$ (1). A crystal measuring 0.50 × 0.20 × 0.20 mm was glued to the end of a glass fiber. No decay of the intensity of the standard was observed and no absorption correction was performed on these data. Because the Hg atom was located at an inversion center, only half of the molecule was located in the asymmetric unit. The final data to parameter ratio was 18:1.

Structure of $[Hg(TMPA)Cl]_2(HgCl_4)$ (2). The crystal measured 0.40 × 0.30 × 0.13 mm. The intensity of the standards decreased about 10% during data collection, and all data were scaled on the basis of the standards. Ψ-curves showed significant variation (65%), and a semiempirical absorption correction was applied to the data. The final data to parameter ratio was 20:1.

NMR Measurements. All solutions for NMR analysis were prepared by adding stock solutions of TMPA in acetonitrile-d_3 to a solution of mercuric perchlorate or mercuric chloride in acetonitrile-d_3 using calibrated autopipets. NMR spectra were recorded in 5-mm-o.d. NMR tubes on a General Electric QE-300 operating in the pulse Fourier transform mode. The sample temperature was maintained by blowing chilled air over the NMR tube in the probe. The variable-temperature unit was calibrated with methanol as previously described.[23] Chemical shifts were measured relative to an internal solvent but are reported relative to tetramethylsilane.

Results

The structures of $[Hg(TMPA)_2](ClO_4)_2$ (**1**) and $[Hg(TMPA)Cl]_2(HgCl_4)$ (**2**) are reported herein. Selected bond distances are given in Table 2 and selected bond angles in Table 3. Thermal ellipsoid plots[21] are shown in Figures 1 and 2, and complete atom labeling schemes are shown in Figures S1−S3. [Note: All figure numbers preceded by "*S*" denote Supporting Information.]

Crystal Structure of $[Hg(TMPA)_2](ClO_4)_2$ (1). The Hg(II) ion is located at an inversion center within a bicapped trigonal antiprism of nitrogen atoms (D_{3d} core symmetry, D_3 ion symmetry). The $Hg-N_{amine}$ distance is nearly the same as the average $Hg-N_{pyridyl}$ distance ($\Delta = 0.02$ Å). Gultneh reports the structure of $[Mn(TMPA)_2](ClO_4)_2$ and describes the six pyridyl nitrogens as forming a distorted octahedron, flattened by 14.9°.[15] Although $[Hg(TMPA)_2]^{2+}$ can be similarly described, an alternate description of the core would put the eight nitrogens at the corners of a distorted cube with intraligand N−N distances of 2.78(2) Å, interligand N−N distances of 3.18(1) Å, and N−N−N angles ranging from 80 to 95° (Figure S4).

This complex appears to be the first example of a structurally characterized eight-coordinate Hg(II) complex in which all the donor nitrogens are part of chelating organic ligands. The three pyridyl ring planes of each ligand are twisted 20.8° on average with respect to the 3-fold axis. The two ligands twist in opposite directions such that H_a and H_b of each pyridyl group are placed directly above the pyridine planes from the opposite part of the molecular ion. The pyridyl ring planes of the manganese complex are twisted about the 3-fold axes in a fashion similar to that in the mercury complex.[15] An eight-coordinate TMPA complex of sodium has also been proposed in which twisting

Table 3. Selected Bond Angles (deg) in $[Hg(TMPA)_2](ClO_4)_2$ and $[Hg(TMPA)Cl]_2(HgCl_4)$

$[Hg(TMPA)_2](ClO_4)_2$		$[Hg(TMPA)Cl]_2(HgCl_4)$	
N−Hg−N(1)	65.93(9)	N(1)−Hg(1)−N(A)	72.5(3)
N−Hg−N(2)	64.63(12)	N(2)−Hg(1)−N(A)	72.0(3)
N−Hg−N(3)	65.69(9)	N(3)−Hg(1)−N(A)	71.8(3)
N−Hg−N(1)[a]	114.07(9)	N(4)−Hg(2)−N(B)	72.3(3)
N−Hg−N(2)[a]	115.37(12)	N(5)−Hg(2)−N(B)	70.5(3)
N−Hg−N(3)[a]	114.31(9)	N(6)−Hg(2)−N(B)	70.3(3)
N(1)−Hg−N(2)	104.01(12)	N(2)−Hg(1)−N(1)	108.6(3)
N(1)−Hg−N(3)	103.38(14)	N(3)−Hg(1)−N(1)	113.9(3)
N(2)−Hg−N(3)	104.32(13)	N(2)−Hg(1)−N(3)	110.4(3)
N(1)−Hg−N(2)[a]	75.99(12)	N(4)−Hg(2)−N(5)	109.7(3)
N(1)−Hg−N(3)[a]	76.62(14)	N(4)−Hg(2)−N(6)	110.7(3)
N(2)−Hg−N(3)[a]	75.68(13)	N(6)−Hg(2)−N(5)	109.5(3)
		Cl(1)−Hg(1)−N(A)	176.7(2)
		Cl(1)−Hg(1)−N(1)	105.1(2)
		Cl(1)−Hg(1)−N(2)	111.1(2)
		Cl(1)−Hg(1)−N(3)	107.7(2)
		Cl(2)−Hg(2)−N(B)	171.6(2)
		Cl(2)−Hg(2)−N(4)	116.0(2)
		Cl(2)−Hg(2)−N(5)	103.9(2)
		Cl(2)−Hg(2)−N(6)	106.7(2)
$Hg-N-C(E)_{av}$	116.0(3)	$Hg-N-C(E)_{av}$	115.9(11)
$Hg-N-C(F)_{av}$	108.5(14)	$Hg-N-C(F)_{av}$	107.0(14)
$Hg-N-C(A)_{av}$	124.3(11)	$Hg-N-C(A)_{av}$	122.9(9)
$C(A)-N-C(E)_{av}$	118.5(4)	$C(A)-N-C(E)_{av}$	120.7(9)
		$Cl-Hg-Cl_{av\ in\ anion}$	109(5)

[a] Symmetry transformation used to generate equivalent atoms is $-x$, $-y + 1$, $-z + 1$.

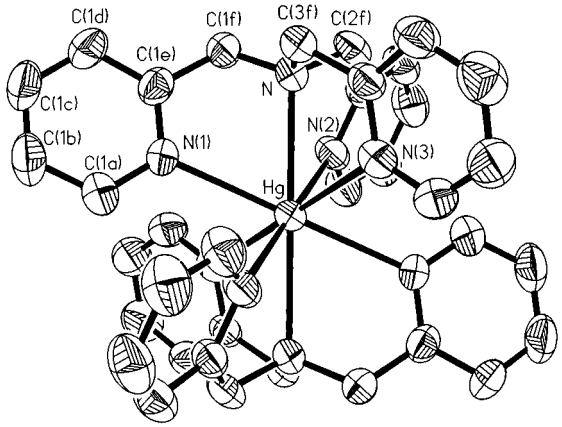

Figure 1. Thermal ellipsoid plot[21] of $[Hg(TMPA)_2]^{2+}$. Ellipsoids are at 50% probability. Hydrogens are omitted for clarity. Only one (2-pyridyl)methyl group has been completely labeled.

(21) *SHELXTL-Plus*, Version 4.21/V; Siemens Analytical X-ray Instruments, Inc.: Madison, WI, **1990**.
(22) Sheldrick, G. M. In *Crystallographic Computing 6*; Flack, H. D., Parkanyi, L., Simon, K., Eds.; Oxford University Press: Oxford, U.K., 1993; p 111.
(23) Raiford, D. S.; Fisk, C. L.; Becker, E. D. *Anal. Chem.* **1979**, *51*, 2050.

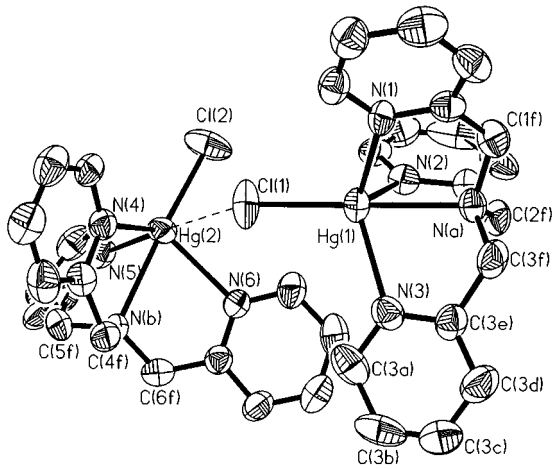

Figure 2. Thermal ellipsoid plot[21] of the two $[Hg(TMPA)Cl]^+$ ions in the asymmetric unit. Ellipsoids are at 50% probability. Hydrogens are omitted for clarity. Only one (2-pyridyl)methyl group has been completely labeled.

of all six pyridyls in the same direction places H_d directly above the pyridine planes of the opposing ligand.[24]

Crystal Structure of $[Hg(TMPA)Cl]_2(HgCl_4)$ (2). There are two $[Hg(TMPA)Cl]^+$ ions and a nearly tetrahedral $[HgCl_4]^{2-}$ anion in the asymmetric unit. The TMPA ligand is tetradentate and the chloride is *trans* to the amine nitrogen, thus forming a distorted trigonal bipyramid. The Hg(II) ion is displaced an average of 0.76(4) Å below the plane of the three pyridyl nitrogens (C_{3v} core symmetry, C_3 ion symmetry). [Tris(2-(dimethylamino)ethyl)amine]cobalt(II) bromide forms a similar ion, with the Co(II) ion displaced 0.32 Å below the equatorial plane.[25] As shown in Figure 2, the two cations are not identical. The packing of these cations places Cl(1) along a line nearly trans (170°) to Hg−N(5) of cation B. The Hg(2)−Cl(1) distance of 3.71 Å is significantly greater than the sum of the van der Waals radii (3.3 Å), however, and the effect on the coordination geometry is small. The Cl(2)−Hg(2)−N(B) angle is decreased by about 5° relative to Cl(1)−Hg(1)−N(A) and the Cl(2)−Hg(2)−N(4) angle is increased by about 5° relative to Cl(1)−Hg(1)−N(2). As in $[Hg(TMPA)_2]^{2+}$, the $Hg-N_{amine}$ distance is nearly the same as the average $Hg-N_{pyridyl}$ distance (Δ = 0.03 Å). The Hg−N distances in $[Hg(TMPA)Cl]^+$ are 0.1 to 0.2 Å shorter than the Hg−N distances in $[Hg(TMPA)_2]^{2+}$. The average Hg−Cl distance of 2.354(12) Å in the cation is consistent with the Hg−Cl distances found in dichlorobisphenoxathiinmercury(II) (2.33 Å)[26] and the dichloro-1-methylcytosinemercury(II) dimer (2.322 Å).[27]

Investigation of TMPA Coordination of Hg(II) in the Solution State. To investigate the solution structure of the TMPA complexes of Hg(II), solutions containing known molar ratios of TMPA and either $Hg(ClO_4)_2$ or $HgCl_2$ in CD_3CN were examined by ^1H and ^{13}C NMR. Selected proton NMR spectra are shown in Figure 3. The chemical shifts of the individual ^1H and ^{13}C resonances as a function of [Hg(II)]/[TMPA] are shown in Figures 4, 5, and S5. The NMR spectra of **1** and **2** were identical to those of the equivalent samples prepared in situ.

The prevalence of rapid exchange in solution state Hg(II) coordination chemistry makes several features of these spectra very notable. Two distinct ligand environments with single ^1H and ^{13}C chemical shifts for all symmetry-related nuclei were

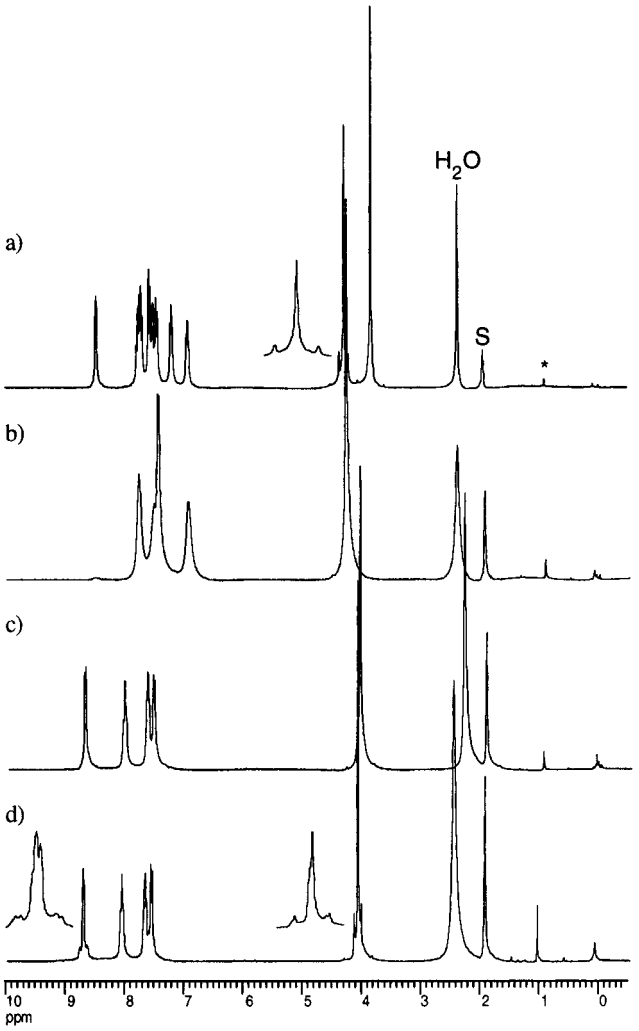

Figure 3. Proton NMR spectra recorded at selected ratios of $Hg(ClO_4)_2$ to TMPA in CD_3CN at 20 °C. The concentration of $Hg(ClO_4)_2$ was fixed at 25 mM. $[Hg(ClO_4)_2]/[TMPA]$ = (a) 0.25, (b) 0.5, (c) 1.0, (d) 1.5. S = CH_3CN; * = impurity.

observed in the presence of 0.125−0.375 equiv of $Hg(ClO_4)_2$ at 20 °C (Figure 3a). The chemical shifts for one set of ^1H and ^{13}C resonances were very similar to those for free ligand and decreased in intensity as the equivalents of $Hg(ClO_4)_2$ were increased. The second set of ^1H resonances increased in intensity as the equivalents of $Hg(ClO_4)_2$ were increased and exhibited $^3J(^1H^{199}Hg)$ of 46 Hz for the H_f protons. Three-bond coupling constants as large as 30 Hz have been reported for the δ- or ϵ-protons of histidine in mercury-substituted proteins.[5] We are aware of only one other synthetic complex of Hg(II) involving exclusively nitrogen donors for which $^3J(^1H^{199}Hg)$ coupling has been observed near room temperature.[28] A summary of all the ^{199}Hg heteronuclear coupling constants observed for the complexes described is provided in Table 4.

The NMR spectra taken at 20 °C exhibited a single set of exchanged-broadened resonances between 0.5 and 1.0 equiv of $Hg(ClO_4)_2$ when the total Hg(II) concentration was 25 mM. The chemical shifts of these resonances changed rapidly with increasing equivalents of Hg(II), and no $^1H^{199}Hg$ couplings were observed until $[Hg(ClO_4)_2]$ was greater than [TMPA]. Slow-exchange conditions for the ^{199}Hg-coupled environment prevalent below 0.5 equiv of $Hg(ClO_4)_2$ were established with a total Hg(II) concentration of 2 mM at 20 °C. Under the latter

(24) Toftlund, H.; Ishiguro, S. *Inorg. Chem.* **1989**, *28*, 2236.
(25) Di Vaira, M.; Orioli, P. L. *Inorg. Chem.* **1967**, *6*, 955.
(26) McEwen, R. S.; Sim, G. A. *J. Chem. Soc. A* **1969**, 1897.
(27) Authier-Martin, M.; Beauchamp, A. L. *Can. J. Chem.* **1977**, *55*, 1213.
(28) Schlager, O.; Wieghardt, K.; Grondey, H.; Rufi'nska, A.; Nuber, B. *Inorg. Chem.* **1995**, *34*, 6440.

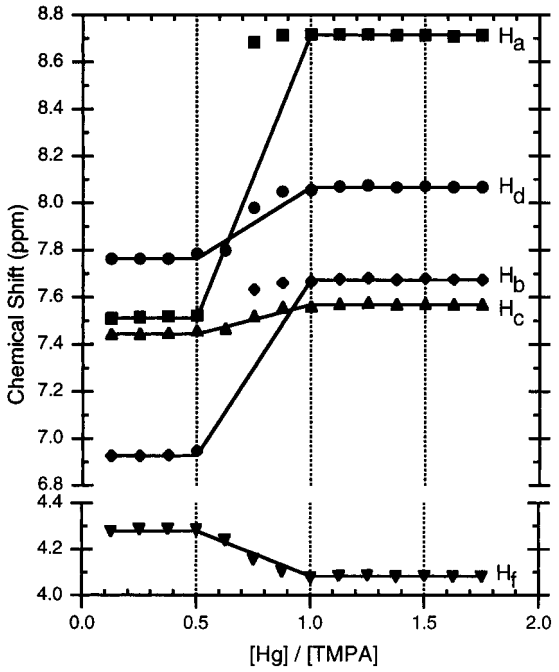

Figure 4. Chemical shifts of protons of TMPA as a function of the $Hg(ClO_4)_2$-to-TMPA ratio in CD_3CN at 20 °C. Chemical shifts associated with a second ligand environment consisting primarily of free ligand in the region below [Hg]/[TMPA] = 0.5 are omitted for clarity. The concentration of $Hg(ClO_4)_2$ was fixed at 25 mM. The lines represent the chemical shifts expected if only $[Hg(TMPA)_2]^{2+}$ and $[Hg(TMPA)]^{2+}$ were present in solution and the equilibrium constant for reaction 3 was large.

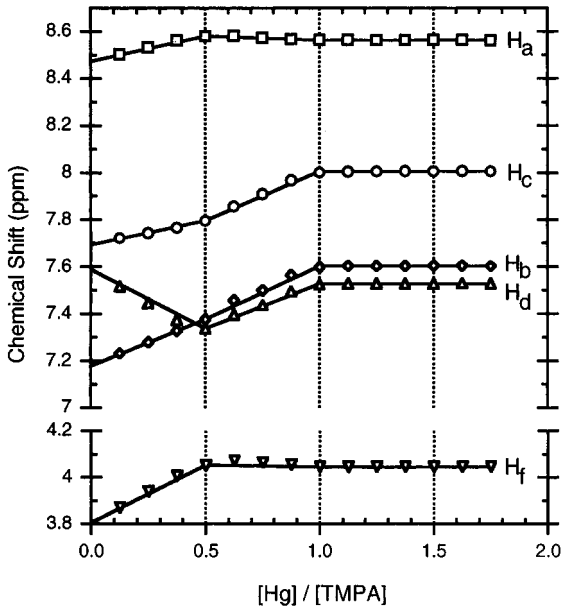

Figure 5. Chemical shifts of protons of TMPA as a function of the $HgCl_2$-to-TMPA ratio in CD_3CN at 20 °C. The concentration of $HgCl_2$ was fixed at 2 mM. The lines represent the chemical shifts expected if the equilibrium constants for formation of $[Hg(TMPA)_2]^{2+}$ and $[Hg(TMPA)Cl]^{+}$ were large and there were no intervening complexes.

conditions, the resonances associated with the coupled environment diminished in intensity and were replaced by a new set of resonances which were distinct from those of free ligand (Figure S6). An additional minor ligand environment was suggested by resonances at 4.1 and 8.5 ppm throughout the transition zone in the 2 mM Hg(II) titrations.

With greater than 1.0 equiv of $Hg(ClO_4)_2$, a single set of ligand resonances with $^3J(^1H^{199}Hg)$ of 40 and 36 Hz for the H_a and H_f protons, respectively, and $^4J(^1H^{199}Hg)$ of 20 Hz for the H_d protons was observed. The complex $[Hg(TMPA)](ClO_4)_2$ (**4**) is proposed to account for the latter observations although we have not yet been able to isolate this complex for structural analysis. For the purposes of this discussion, we are not making a distinction between **4** and a solvate such as $[Hg(TMPA)NCCH_3](ClO_4)_2$. The presence of at least one additional ligand is characteristic of the reported solid state structures of TMPA metal complexes with noncoordinating counterions.[7−19] Furthermore, completion of the coordination sphere of the cation by the more coordinating solvent acetonitrile may partially explain the inability to detect $J(^1H^{199}Hg)$ couplings in spectra recorded under identical conditions in acetone-d_6. The couplings reported here accounted for approximately 17% of the area of each resonance as expected on the basis of the natural abundance of ^{199}Hg. The size and shape of the mercury satellites were unaffected by a 2-fold excess of Hg(II) with total concentrations of $Hg(ClO_4)_2$ at or below 25 mM. At significantly higher total concentrations of $Hg(ClO_4)_2$, the satellite peaks broadened with excess metal while all other lines remained sharp, suggesting exchange between **4** and excess metal on the NMR time scale.

Table 4. Summary of ^{199}Hg Heteronuclear Coupling Constants Observed and Putative Assignments[a]

	$J(^1H^{199}Hg)$, Hz			$J(^{13}C^{199}Hg)$, Hz		
compound	H_a	H_d	H_f	C_b	C_d	C_f
$[Hg(TMPA)_2](ClO_4)_2$ (**1**)[b]			46	30	44	26
$[Hg(TMPA)Cl]Cl$[c]	24		45			
$[Hg(TMPA)](ClO_4)_2$ (**4**)[b]	40	20	36	32	42	30

[a] Determined at 20 °C in acetonitrile-d_3. [b] Concentration of complex ≤ 25 mM. [c] Concentration of complex ≤ 2 mM.

The trends in the ^{13}C chemical shifts of the ligand with increasing equivalents of $Hg(ClO_4)_2$ paralleled those observed in the ^1H spectra. The most notable features of these solution spectra were the $J(^{13}C^{199}Hg)$ couplings. The vast majority of previously reported $^{13}C^{199}Hg$ couplings have been for alkylmercurials which follow the usual rules for heavy-nucleus coupling constants: $^1J \gg {}^3J > {}^2J$.[29] With 0.125−0.375 equiv of $Hg(ClO_4)_2$, 30, 44, and 26 Hz three-bond couplings with the C_b, C_d, and C_f carbons, respectively, of TMPA were observed. $^{199}Hg-{}^{13}C$ coupling constants of similar magnitude for these ^{13}C atoms were also observed in samples with [Hg(II)] ≥ [TMPA] but not at intermediate Hg(II) stoichiometries with 25 mM total $Hg(ClO_4)_2$ samples. Each of the $J(^{13}C^{199}Hg)$ values observed apparently arose from $Hg-N_{py}-C_x-C_y$ three-bond coupling. Three-bond coupling to C_e through the $Hg-N_{amine}-C_f-C_e$ bonds was not observed. Significantly, a normal Karplus-type relationship for the magnitudes of $^3J(^{13}C^{199}Hg)$ predicts weak three-bond coupling for torsion angles close to 90° and the largest three-bond couplings for torsion angles that approach 0 or 180°.[30] In **1** and **2**, the average torsion angle between Hg and C_e was 45°, while the average torsion angles between Hg and C_b, C_d, and C_f were within 15° of either 0 or 180°. Evidence for a Karplus-type relationship for the magnitudes of $^3J(^1H^{199}Hg)$ has been reported.[4]

The spectra described above support formation of exchange-inert cations in acetonitrile solutions of Hg(II) and TMPA with stoichiometies of 1:2 and 1:1 as found for complexes **1** and **2**. Rapid intramolecular exchange processes which interconvert symmetry-related 2-methylpyridyl arms of the TMPA ligand(s) would be expected in solution for cations resembling those found in either **1** or **2**. Full analysis of the complementarity

(29) (a) Wrackmeyer, B.; Contreres, R. *Annu. Rep. NMR Spectrosc.* **1992**, *24*, 267. (b) Granger, P. In *Transition Metal Nuclear Magnetic Resonance*; Pregosin, P. S., Ed.; Elsevier: New York, 1991; p 306.
(30) Karplus, M. *J. Chem. Phys.* **1959**, *30*, 11.

between the solution state NMR spectra and the solid state structures is reserved for the Discussion.

Detailed analysis of the spectra acquired as a function of metal-to-ligand ratio revealed a series of linked equilibria. Reactions 1 and 2 describe the prevalent equilibria at metal-

$$Hg^{2+} + TMPA \rightleftharpoons [Hg(TMPA)]^{2+} \quad (1)$$

$$[Hg(TMPA)]^{2+} + TMPA \rightleftharpoons [Hg(TMPA)_2]^{2+} \quad (2)$$

to-ligand stoichiometries lower than 0.5. The equilibrium of reaction 2 lies extremely far to the right with $Hg(ClO_4)_2$, since exchange of **1** with all other TMPA-containing species approaches the slow-exchange limit (Figure 3a). The second set of ligand resonances present at the low end of the titration drifts only slightly from the resonances of the free ligand toward the resonances associated with **4** (Figure S6), suggesting reaction 1 has a much lower equilibrium constant than reaction 2.

At metal-to-ligand stoichiometries between 0.5 and 1, severely exchanged broadened ligand resonances were observed with 25 mM $Hg(ClO_4)_2$-containing samples. The fast-exchange limit could be approached for most resonances by making the total $Hg(ClO_4)_2$ concentration greater than 100 mM (data not shown). The slow-exchange limit between **1** and all other TMPA-containing species could be established in this region with a total $Hg(ClO_4)_2$ concentration of 2 mM (Figure S6). Formation of a 1:1 cation similar to those in **2** (e.g., $[Hg(TMPA)](ClO_4)_2$ (**4**)) could occur directly from **1** cations according to reaction 3. Assuming the cations of **1** and **4** were the only TMPA-

$$[Hg(TMPA)_2]^{2+} + Hg^{2+} \rightleftharpoons 2[Hg(TMPA)]^{2+} \quad (3)$$

containing species in solution, the observed chemical shift of the exchange-averaged resonances should be given by expression 4 where the weighted averages of the chemical shifts of

$$\delta_{obs} = P_{1:1}\delta_{1:1} + (1 - P_{1:1})\delta_{1:2} \quad (4)$$

the species present in solution are δ_{obs}, $\delta_{1:1}$, and $\delta_{1:2}$ and $P_{1:1}$ and $P_{1:2}$ [$=0.5(1 - P_{1:1})$] are the mole fractions of **1** and **4**, respectively.[1] If the equilibrium of reaction 3 lies far to the right, then the lines in Figure 4 represent the expected trends of the chemical shifts. On the other hand, if the equilibrium of reaction 3 does not lie far toward product formation, smooth curves which only approach the lines at a molar ratio greater than 1 are expected. Although the error in the chemical shift recorded in the transition region might be as large as 0.05 ppm because the reported spectra were not taken at the fast-exchange limit, deviations as large as 0.5 ppm above the ideal curve strongly suggest involvement of another TMPA-containing species in the interconversion of **1** and **4**.

To further characterize the interconversion of these two complexes, acetonitrile solutions were cooled to −40 °C. In the transition zone between 0.5 and 1.0 equiv of $Hg(ClO_4)_2$, **1** and **4** appeared to be the major components. Minor ligand resonances distinct from those attributed to **1**, **4**, and free TMPA were detectable at −40 °C with a total $Hg(ClO_4)_2$ concentration of 25 mM. Considerable broadening at −40 °C precluded quantitation of the complexes and determination of relevant equilibrium constants in acetonitrile. Additional studies done in acetone-d_6 at temperatures as low as −90 °C suggested much more complicated equilibria (data not shown).

Several multinuclear species are plausible for interconversion of **1** and **4**. A complex of stoichiometry Hg_2TMPA_3 (**5**) with each Hg(II) coordinated to all four nitrogens of one TMPA and additional coordination by a TMPA bridging two metal ions is an obvious candidate. This stoichiometry is also suggested by the appearance of resonances indistinguishable from those of **4** above 0.675 equiv of Hg(II) in titrations done with 2 mM $Hg(ClO_4)_2$ (Figure S6). Interestingly, ^{199}Hg heteronuclear coupling to **1** is constant in magnitude and intensity throughout the transition region from 0.5 to 1.0 equiv of $Hg(ClO_4)_2$ in the latter titrations but absent in the set of proton resonances attributed to **4**. This suggests there must be a mechanism for rapid exchange between the various pyridyl environments of $Hg_2(TMPA)_3$ and **4**. We propose that transient formation of $Hg_3(TMPA)_4$ (**6**) by reaction 5 would lead to the observed exchange

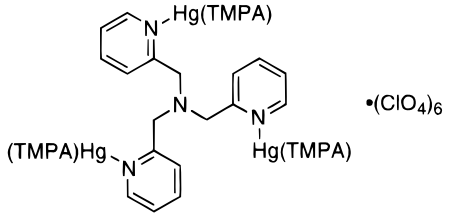

6

$$[Hg_2(TMPA)_3]^{4+} + [Hg(TMPA)]^{2+} \rightleftharpoons [Hg_3(TMPA)_4]^{6+} \quad (5)$$

decoupling. Cooling to −40 °C slowed the exchange decoupling process for **4** on the NMR time scale in solutions containing a total of 2 mM $Hg(ClO_4)_2$.

A wide variety of multinuclear complexes involving TMPA have been structurally characterized; however, to our knowledge, none of them involve a metal-bridging TMPA. The similarity of the environments of the nonbridging ligands in **1**, **5**, and **6** would likely lead to similar ^1H NMR resonances. Complexes **5** and **6** are apparently minor components of the equilibrium mixture, and most of the resonances associated with the bridging ligands are either obscured by other resonances or are too small to be detected. Additional indirect support for at least one multinuclear intervening species was provided by experiments at higher concentrations, which permitted spectra to be recorded near the fast-exchange limit. Deviations from the behavior predicted for reaction 3 were much smaller at higher concentration, apparently due to the effect of Le Châtalier's principle on coupled equilibria such as (6) and (7).

$$[Hg(TMPA)_2]^{2+} + [Hg(TMPA)]^{2+} \rightleftharpoons [Hg_2(TMPA)_3]^{4+} \quad (6)$$

$$[Hg_2(TMPA)_3]^{4+} + Hg^{2+} \rightleftharpoons 3[Hg(TMPA)]^{2+} \quad (7)$$

For comparison, the coordination properties of TMPA were also investigated with chloride counterions and total Hg(II) concentrations of 2 and 25 mM (Figures 5, S7, and S8). In the 2 mM Hg(II) samples, the chemical shift discontinuities observed at [Hg]/[TMPA] of 0.5 and 1.0 supported the existence of a series of linked equilibria similar to those in the perchlorate system (Figure 5). However, the magnitude of all the equilibrium constants was clearly reduced. Significantly higher total Hg(II) concentrations shifted these discontinuities to higher [Hg]/[TMPA] ratios and masked all $J(^1H^{199}Hg)$ couplings (Figure S7). In contrast to the perchlorate system, free ligand exchanged rapidly with the ligands of $[Hg(TMPA)_2]^{2+}$ at 20 °C at the concentrations examined. Cooling to −40 °C provided two sets of ligand resonances with 0.125−0.375 equiv of $HgCl_2$, one of which resembled those of the free ligand, but residual exchange broadening precluded detection of ^{199}Hg coupling to the other set. Interestingly, the chemical shifts of H_a and H_b of $[Hg(TMPA)_2]^{2+}$ in the chloride system differ by 1.07 and 0.45 ppm,

respectively, from those observed in the perchlorate system. These differences are further elaborated in the Discussion.

Multinuclear intermediates were also implicated in the exchange of TMPA between 1:2 and 1:1 metal-to-ligand complexes in the chloride system. Although the chemical shift varied essentially linearly in the transition zone from 0.5 to 1.0 equiv of Hg(II) at 20 °C with a 2 mM total $HgCl_2$ concentration, marked curvature was apparent at −40 °C (Figure S8). The end point of this titration in acetonitrile appears to be $[Hg(TMPA)Cl]^+$ (**7**), the proton chemical shifts of which are all shifted upfield compared to those of **4**, but by no more than 0.13 ppm. This cation exhibited $^3J(^1H^{199}Hg)$ values of 45 and 24 Hz for the H_a and H_f protons, respectively.

Discussion

Anderegg and co-workers have reported stability constants

$$\beta_1 = [M(TMPA)]/[M][TMPA] \quad (8)$$

and

$$\beta_2 = [M(TMPA)_2]/[M][TMPA]^2 \quad (9)$$

for TMPA with the nitrate salts of nine and two divalent metal ions in aqueous solution, respectively.

Mercury(II) had the largest values of both $\log \beta_1 = 17.15$ and $\log \beta_2 = 24.10$, and these are probably representative of the values for the perchlorate system and much higher than the values for the chloride system. Interestingly, the manganese complex mentioned above appears to be the only previously structurally characterized complex of the type $[M(TMPA)_2]^{n+}$ although $\log \beta_2$ was not reported by Anderegg.[15] A wide variety of complexes of the type $[M(TMPA)]^{n+}$ are known with various other ligands completing the coordination sphere of the metal.

The NMR titration experiments reported here are consistent with TMPA having large values of both β_2 and β_1 for complexes of $Hg(ClO_4)_2$ and $HgCl_2$, with $\beta_2 \gg \beta_1$. Formation of a complex of the type $[M(TMPA)_2]^{2+}$ was strongly suggested by the ability to observe a single new ligand environment that exchanged slowly with all other TMPA-containing species present relative to the NMR time scale in spectra with less than 0.5 equiv of Hg(II). The new ligand environment exhibited coupling between ^{199}Hg and H_f with perchlorate counterions, which was assigned to **1** as detailed below. With chloride counterions, a related complex was apparently formed with significant differences in chemical shift and no detectable ^{199}Hg coupling, possibly due to residual exchange broadening. The associative process (6) was implicated in exchange of ligand between 1:1 and 1:2 metal-to-ligand complexes on the basis of the concentration dependence of exchange decoupling and the nonlinear change in chemical shift of solutions containing between 0.5 and 1 equiv of Hg relative to TMPA. The magnitude of β_2 in both counterion systems apparently precludes significant involvement of a dissociative mechanism in ligand exchange. Slow exchange relative to the NMR time scale was established for 1:1 metal-to-ligand complexes when [Hg(II)] ≥ [TMPA]. The chemical shifts of the 1:1 metal-to-ligand complexes were very similar, and ^{199}Hg coupling to ligand nuclei was detected in both counterion systems.

On the basis of our data, it was clear that the equilibrium constants for formation of the 2:1 metal-to-ligand complexes were much greater than the net equilibrium constants for formation of the 1:1 metal-to-ligand complexes and both of these were greater than the net equilibrium constants for formation of the multinuclear intermediates. At metal-to-ligand ratios below 0.5, the ^1H and ^{13}C chemical shifts for the ligand that were not associated with $[Hg(TMPA)_2]^{2+}$ were generally observed to drift toward the chemical shifts of the 1:1 metal-to-ligand complex (Figures S6 and S8). Formation of 1:1 metal-to-ligand complexes from $[Hg(TMPA)_2]^{2+}$ without long-lived intermediates is plausible. However, the deviations of the ligand chemical shifts from the curves predicted by eq 4 between 0.5 and 1.0 equiv of Hg(II) (see Figures 4, S5, and S8) require significant involvement of coupled reactions such as (6) and (7) in the formation of **4** and related reactions for the formation of **7**. The 2:3 metal:ligand stoichiometry of the major multinuclear intermediate is suggested by the appearance of resonances indistinguishable from those of the 1:1 metal-to-ligand complexes above 0.675 equiv of Hg(II) in titrations done with 2 mM Hg(II) (Figures S6 and S8). Direct formation of multinuclear complexes such as **5** from the free ligand through a pentamolecular process is unlikely for entropic reasons. At higher total metal concentration, the constraint of the small equilibrium constant for reaction 6 was reduced and the chemical shifts were much closer to the predicted curves.

Significantly, the solution state NMR spectra below 0.5 equiv of Hg(II) were consistent with the solid state structure reported for $[Hg(TMPA)_2](ClO_4)_2$. While correlations between solid state structures and solution state NMR properties must always be made cautiously,[31] compelling evidence for formation of **1** in solution is provided by a combination of symmetry, shielding, and heteronuclear coupling arguments. The six 2-methylpyridyl ligand arms were nearly equivalent in the solid state structure with D_{3d} symmetry. A total of six ^1H resonances and six ^{13}C resonances could be anticipated on the basis of the solid state structure. Six ^{13}C resonances but only five proton resonances in a 1:1:1:1:2 ratio were observed, suggesting that the H_f protons both had chemical shifts of 4.28 ppm in the solution state structure. The H_f protons of **1** continued to exhibit a single, sharp resonance at −40 °C. An NMR spectrum for the paramagnetic $[Mn(TMPA)_2](ClO_4)_2$ complex was not reported. Several complexes of the type M(TMPA) with significantly lower overall symmetry have been reported as having distinct resonances for the methylene protons.[7,18]

The chemical shift equivalence of the methylene protons of $[Hg(TMPA)_2]^{2+}$ in the solution state could arise by accidental degeneracy; however, a single chemical shift for the H_f protons of both **4** and **7** suggests alternatives be considered. For example, relaxation of the twist angle between the pyridyl ring planes and the 3-fold axis would relate the protons by a mirror plane. Alternatively, the methylene protons could exhibit an average chemical shift due to an effective inversion about the amine nitrogen associated with rocking of the pyridyl rings with respect to the 3-fold axes on a time scale rapid compared to the NMR time scale. A rocking motion which changes the orientation of the shielding ring current of the pyridine planes with respect to the opposite ligand would provide a plausible explanation for the upfield shifts of 0.95 and 0.25 ppm, respectively, for H_a and H_b in the ^1H NMR and the weaker upfield shift of 0.14 ppm for the more distant H_d in $[Hg(TMPA)_2](ClO_4)_2$ relative to free ligand. The most striking feature of the ^1H NMR spectra of the putative $[Na(TMPA)_2]^+$ complex was an estimated upfield shift of 0.37 ppm for H_d relative to free ligand proposed to be due to interactions with the ring current of the opposing ligand.[24] In contrast, the H_f and H_c protons of **1** exhibited downfield shifts of 0.47 and 0.08 ppm, respectively, which is a common result of the deshielding influence of σ donation to a metal cation. The ^{13}C spectrum of **1** also exhibited large upfield and downfield differences from

(31) Davies, J. A.; Dutremez, S. *Coord. Chem. Rev.* **1992**, *114*, 201.

free TMPA which seemed to correspond to parts of the ligand that were more distal or proximal, respectively, to the metal ion.

The final piece of evidence correlating the solution state spectra with the solid state structure of **1** is the intensity of $^3J(^1H^{199}Hg)$. Coupling satellites were observed to account for a total of approximately 17% of the main H_f resonance. This is most consistent with the limited dihedral angle range available to the H_f protons when all the nitrogens of the coordinating ligands have significant bonding interactions with the metal center.

Intriguingly, in the chloride system there is still a single set of five ^1H resonances for the methylpyridyls in the spectra assigned to $[Hg(TMPA)_2]Cl_2$, but only that of H_d is shifted upfield relative to free ligand. Strong upfield shifts of only the H_d resonace is reminiscent of the spectrum attributed to $[Na(TMPA)_2]ClO_4$, proposed to involve parallel alignment of the pyridyls from opposing ligands.[24] Unfortunately, we were not able to detect ^{199}Hg coupling to the ligand nuclei of this complex under any conditions, so structural correlations are tentative. Alternative structures with pendant pyridyls, possibly involving significant bonding interaction between the metal ion and one or more counterions, are plausible.

In contrast, the proton chemical shifts for the complexes prevalent in the presence of ≥ 1 equiv of Hg were essentially unchanged or shifted downfield by 0.5 ppm or less with respect to free ligand. Cations of stoichiometry $[Hg(TMPA)]^{2+}$ (**4**) and $[Hg(TMPA)Cl]^+$ (**7**) were proposed as being consistent with the data. If ion pairing to form **2** is occurring to a significant extent under the conditions examined in the chloride system, it has essentially no impact on either the chemical shifts or the coupling constants of **7**. Downfield shifts with respect to the free ligand for all protons in **4** and **7** are anticipated since shielding from another ligand molecule would not be experienced. The upfield and downfield differences in each ^{13}C chemical shift with respect to free TMPA were enlarged in **4** compared to **1**. The only exception to this observation was C_a. Weakly shielded with respect to free TMPA in **1**, C_a was deshielded in **4**, possibly due to loss of shielding from the opposite ligand. Carbon spectra are unavailable for **7** because of concentration constraints, but the ^{13}C chemical shifts of 25 mM $HgCl_2$ samples were approaching those of **4** at high [Hg]/[TMPA] ratios (data not shown). The ^{199}Hg coupling constants with ligand nuclei observed for **4** and **7** were comparable in magnitude to those believed to be associated with **1** as described above. Small couplings to additional pyridyl protons (H_a and H_d) were detected upon reduction in the apparent mercury coordination number from 8 to 4 or 5.

The ^1H chemical shifts of **4** and **7** were similar. Higher metal electron density with chloride counterions was suggested by the smaller chemical shift differences between free ligand and all ligand resonances in the 1:1 metal-to-ligand cations of **7** compared to **4**. This suggests that σ donation is less prevalent in **7**. Interestingly, the magnitudes of $^3J(^1H^{199}Hg)$ for **7** are intermediate to the values attributed to **1** and **4**. Literature precedent for ^{199}Hg coupling in coordination compounds is currently too limited to draw extensive structural conclusions.

Conclusions

We have demonstrated that heteronuclear coupling to ^{199}Hg facilitates the analysis of the complex equilibria involved in Hg(II) coordination to a potentially tetradentate ligand. Cations of stoichiometry $[Hg(TMPA)_2]^{2+}$, and $[Hg(TMPA)]^{2+}$ and $[Hg(TMPA)Cl]^+$ were characterized by ^1H and ^{13}C NMR in acetonitrile. Conditions under which these cations were exchange-inert on the NMR time scale were established at metal-to-ligand ratios either below 0.5 or above 1. Nuclei of the ligands of these cations exhibited heteronuclear coupling to ^{199}Hg at room temperature. An additional complex with stoichiometry $[Hg_2(TMPA)_3]^{4+}$ was proposed for exchange of ligand between 1:1 and 1:2 metal-to-ligand complexes to explain deviations from the predicted chemical shift as a function of [Hg(II)]/[TMPA].

The potentially tetradentate, tripodal ligand TMPA coordinated to Hg(II) with essentially 3-fold symmetry under the conditions examined. The crystal structures of **1** and **2** revealed only slight differences between each of the 2-methylpyridyl arms of the complexes. In solution, these differences were not apparent in the ^1H and ^{13}C NMR spectra of individual complexes due to intramolecular exchange processes. In the future, the sensitivity of the tremendous chemical shift dispersion of ^{199}Hg to intramolecular vibrational fluctuations may be investigated by comparisons of the solution state ^{199}Hg chemical shifts of these and related complexes to their isotropic solid state chemical shifts.

Cations believed to have ligand geometries comparable to those of **1** and **2** in solution exhibited trends in the magnitudes of $^3J(^{13}C^{199}Hg)$ consistent with a Karplus-type relationship. Recently a Karplus-type relationship was suggested for the magnitudes of $^3J(^1H^{199}Hg)$.[4] Further support for these relationships would permit ^{199}Hg scalar coupling information to be used in future distance geometry-based structure refinement strategies.

The relative ease of interpretation of these solution state spectra should motivate investigation of the mercury coordination chemistry of additional multidentate ligands, including the effect of chelate ring size, steric hindrance, and mixed donor ligands on solution equilibria. Of particular interest is the development of trends in $^1H^{199}Hg$ and $^{13}C^{199}Hg$ coupling constants that can be correlated with the structure of mercury coordination compounds. This study extends literature precedent for enhancing heteronuclear coupling in solution with multidentate ligands by reducing the prevalence of intermolecular exchange processes.[2,3,28,32] However, heteronuclear coupling is not routinely observed with multinuclear ligands,[33] and this work demonstrates that solvent, counterion and concentration, must all be optimized in solution state NMR studies.

Acknowledgment. This research was supported by the Thomas F. and Kate Miller Jeffress Memorial Trust and by the donors of the Petroleum Research Fund, administered by the American Chemical Society. The NSF-ILI program provided funding for the X-ray diffractometer. We thank Dr. Robert D. Pike for helpful discussions and technical review of this paper.

Supporting Information Available: Figures S1−S8, showing thermal ellipsoid plots and additional plots of proton and carbon chemical shifts (8 pages). Two X-ray crystallographic files, in CIF format, are available on the Internet only. Ordering and access information is given on any current masthead page.

IC9702779

(32) McCrindle, R.; Ferguson, G.; McAlees, A. J.; Parvez, M.; Ruhl, B. L.; Stephenson, D. K.; Wieckowski, T. *J. Chem. Soc., Dalton Trans.* **1986**, 2351.
(33) Bryant, L. H.; Lachgar, A.; Jackels, S. C. *Inorg. Chem.* **1995**, *34*, 4230.